JOURNAL OF CLINICAL MICROBIOLOGY, Aug. 2006, p. 2942–2950 Vol. 44, No. 8
0095-1137/06/$08.00+0 doi:10.1128/JCM.00585-06

Evaluation of In Situ Methods Used To Detect *Mycobacterium avium* subsp. *paratuberculosis* in Samples from Patients with Crohn's Disease

Mangalakumari Jeyanathan,[1] David C. Alexander,[1] Christine Y. Turenne,[1] Christiane Girard,[2] and Marcel A. Behr[1]*

McGill University Health Centre, Montreal, Quebec, Canada,[1] and Université de Montréal, Faculté de Médecine Veterinaire, Ste.-Hyacinthe, Québec, Canada[2]

Received 20 March 2006/Returned for modification 10 May 2006/Accepted 5 June 2006

In common with other diagnostic tests, detection of mycobacteria in tissue by microscopic examination is susceptible to spectrum bias. Since Crohn's disease is defined by the absence of detectable pathogenic organisms, the use of in situ techniques to search for *Mycobacterium avium* subsp. *paratuberculosis* in Crohn's disease samples requires validation of methods in a paucibacillary setting. To generate paucibacillary infection, C57BL/6 mice were artificially infected with *Mycobacterium avium* subsp. *paratuberculosis* strain K10 and *M. tuberculosis* H37Rv, yielding tissues harboring fewer than one bacillus per oil immersion field. Serial sections of organs were then studied by cell wall-based staining techniques (Ziehl-Neelsen and auramine rhodamine) and nucleic acid-based staining techniques (in situ hybridization [ISH] and indirect in situ PCR [IS PCR]). Microscopic examination and measurement of morphometric parameters of bacilli revealed that for all methods, *Mycobacterium avium* subsp. *paratuberculosis* bacilli were observed to be shorter, smaller, and less rod shaped than *M. tuberculosis* bacilli. Ziehl-Neelsen, auramine rhodamine stains, ISH targeting rRNA, and IS-PCR targeting the IS*900* element afforded comparable sensitivities, but for all methods, visualization of individual bacterial forms required magnification ×1,000. Auramine rhodamine staining and IS-PCR generated positive signals in negative controls, indicating the nonspecificity of these assays. Together, our results indicate that detection of *Mycobacterium avium* subsp. *paratuberculosis* bacilli in tissue requires oil immersion microscopy, that rRNA-ISH provides sensitivity and specificity comparable to those of Ziehl-Neelsen staining, and that the microscopic detection limit for *Mycobacterium avium* subsp. *paratuberculosis* in tissue is governed more by bacterial burden than by staining method.

For nearly a century, investigators have explored a potential link between *Mycobacterium avium* subsp. *paratuberculosis* and inflammatory bowel disease of humans (8). Efforts have focused particularly on Crohn's disease, largely stimulated by the histopathologic similarity between human Crohn's disease and certain forms of paratuberculosis (13). Although a number of different laboratory methodologies have been employed to search for *Mycobacterium avium* subsp. *paratuberculosis* in Crohn's disease, the published results have been conflicting, resulting in neither confirmation nor rejection of this hypothesis to date (41).

The recent availability of genetic and genomic data for *Mycobacterium avium* subsp. *paratuberculosis* offered promise that molecular diagnostic strategies might overcome the limitations of conventional microbiologic tests for this fastidious organism (45). The insertion element IS*900*, found at 14 to 18 copies per genome, has been widely used as a target for PCR (4–7, 17, 27, 30, 38, 39, 42, 44) and in situ hybridization (19–21, 37, 43), but for both applications, variable results have resulted in as many questions as answers (52). An important limitation of studies looking for novel pathogens is that information about sensitivity and specificity of assays applied is generally lacking. For *Mycobacterium avium* subsp. *paratuberculosis*, the greatest experience resides in laboratories that employ conventional and molecular methods for detecting the organism in cattle and sheep (16, 53). Although these methods can be directly applied to human samples, their utility in a human disease that is defined by the absence of detectable pathogens requires consideration of spectrum bias, both for optimizing techniques and for interpreting the results.

Spectrum bias, also known as spectrum effect, refers to the observation that the operating parameters of a diagnostic assay vary as a function of the disease state (28, 36). The impact of spectrum bias has been well established for the diagnosis of a number of infectious diseases (15, 23), including the mycobacterial diseases leprosy and tuberculosis (TB). In leprosy, the sensitivity of tissue microscopy for acid-fast bacilli depends on the bacterial burden and is therefore greater in lepromatous than tuberculoid disease (31). Likewise, the sensitivity of nucleic-acid-based tests is also influenced by the bacterial burden, as exemplified by the compromised sensitivity of PCR-based assays for sputum smear-negative TB (11, 22, 32). By extension, assays that reliably detect abundant *Mycobacterium avium* subsp. *paratuberculosis* organisms in livestock with Johne's disease may not provide sufficient sensitivity to study human Crohn's tissue.

To date, in situ studies of *Mycobacterium avium* subsp. *paratuberculosis* in Crohn's disease have validated their methods using naturally infected pluribacillary livestock samples (49), tissue blocks artificially injected with high numbers of *Mycobacterium avium* subsp. *paratuberculosis* bacteria (20), or serial dilutions of bacteria in vitro (37). In contrast, an assay for

* Corresponding author. Mailing address: Division of Infectious Diseases and Medical Microbiology, A5-156, Montreal General Hospital, 1650 Cedar Avenue, Montreal, QC H3G 1A4, Canada. Phone: (514) 934-1934, ext. 42815. Fax: (514) 934-8423. E-mail: marcel.behr@mcgill.ca.

TABLE 1. PCR primers and PCR conditions to generate probes and target amplification in tissue for IS*900*-based assays

Target sequence	Primer sequence (5′–3′)	Product size (bp)	PCR conditions	Reference
IS*900* (for probe)	AV1: ATGTGGTTGCTGTGTTGGATGG AV2: CTGGAGTTGATTGCGGCGG	298	35 cycles of 94°C, 1 min; 58°C, 1 min; 72°C, 3 min of 35 cycles plus final extension at 72°C, 3 min	29
IS*900* (for IS-PCR)	L1: CTTTCTTGAAGGGTGTTCGG L2: ATGGAGGCGAGGTCACGT	400	Same, except annealing at 60°C	29

Mycobacterium avium subsp. *paratuberculosis* in Crohn's must be able to specifically detect small numbers of organisms within the tissue, near or below the threshold of microscopic detection. To address this, we have produced artificial mycobacterial infections in mice where the bacterial burden was near the threshold of microscopic detection. The availability of tissue with certain paucibacillary *Mycobacterium avium* subsp. *paratuberculosis* infection permitted us to directly compare the sensitivity of cell wall-based (Ziehl-Neelsen [ZN] and auramine rhodamine) and nucleic acid-based staining (in situ hybridization and indirect in situ PCR) methods. Additionally, tissue from uninfected and *M. tuberculosis*-infected animals permitted us to determine whether these same methods were prone to false-positive results in the absence of *Mycobacterium avium* subsp. *paratuberculosis.*

MATERIALS AND METHODS

Generation of *M. avium paratuberculosis*- and *M. tuberculosis*-infected tissue. As part of separate studies on the relative virulence of *Mycobacterium avium* complex strains and the efficacy of different BCG vaccines, 8-week-old C57BL/6 mice were infected with *Mycobacterium avium* subsp. *paratuberculosis* strain K10 and with *M. tuberculosis* H37Rv. Phosphate-buffed saline (PBS) injections (100 microliters intravenously and intraperitoneally, respectively) provided uninfected control samples from animals housed in separate cages of the same facility. *Mycobacterium avium* subsp. *paratuberculosis*-infected mice were housed in the conventional rodent facility of the McGill University Health Centre Research Institute; *M. tuberculosis* infections were done in our level 3 containment facility, where mice were then housed and subsequently sacrificed. All procedures were approved by the Facility Animal Care Committee as recommended by the Canadian Council on Animal Care. Two separate experiments permitted us to establish the spectrum of bacterial burden in the organs. A total of 10 mice were infected by the intravenous and intraperitoneal routes with *Mycobacterium avium* subsp. *paratuberculosis* strain K10 (1×10^6 CFU in 0.1 ml PBS). Additionally, a group of five mice infected by the intravenous route with virulent *M. tuberculosis* strain H37Rv (1×10^6 CFU in 0.1 ml PBS) and five mice injected with PBS provided us with specificity controls. Finally, to compare the morphology of *Mycobacterium avium* subsp. *paratuberculosis* organisms in our murine infections to that with natural Johne's disease, tissue samples were obtained from culled sheep diagnosed with pluribacillary paratuberculosis based on the presence of granulomatous ileitis, demonstration of bacteria by Ziehl-Neelsen staining in the lesions, and detection of *Mycobacterium avium* subsp. *paratuberculosis*-specific DNA by IS*900*-based PCR.

Determination of CFU in mice organs. At 4 and 8 weeks postinfection, mice were sacrificed by asphyxiation with carbon dioxide gas. For four mice from each experiment group, the spleen, lung, and liver were aseptically removed and weighed prior to processing for quantitative culture. Weighing the whole organ permitted us to calculate the bacterial burden per gram of tissue and thereby to estimate the bacterial burden of the fifth mouse that served for histological examination. Culture determinations followed standard procedures. In brief, organs were homogenized with a Polytron homogenizer (Glen Mills, Inc.) in sterile 50-ml tubes containing 4 ml isotonic saline. Dilutions of each homogenate were spread onto duplicate plates containing Bacto Middlebrook 7H10 agar (Difco) enriched with 10% OADC (oleic acid, bovine serum albumin [fraction V], dextrose, and catalase) (Becton, Dickinson and Company) and mycobactin J (2 μg/ml) (Allied Monitor, Inc.). Plates were incubated at 37°C until colonies appeared, usually after 3 to 6 weeks. The identity of bacterial cultures was confirmed both before injection and after recovery from mice, using strain-specific genetic markers, described elsewhere (45).

Preparation of smears of cultures for cell wall-based and rRNA staining. To estimate the morphometric parameters of bacillus, smears were made on microscopic slides using log-phase culture of *Mycobacterium avium* subsp. *paratuberculosis* strain K10 and *Mycobacterium bovis* BCG Russia. Smears were air dried and heat fixed and then subjected to auramine rhodamine staining. For rRNA staining, aliquots of log-phase cultures were centrifuged at 4,000 rpm for 15 min and washed twice in PBS. Ten microliters of resuspended pellet in PBS was spotted on silane (Sigma-Aldrich)-coated slides and air dried. Smears on the slides were fixed in 10% buffered formalin (Fisher) for 2 to 3 h, washed briefly in PBS, and immersed in ice-cold ethanol for 10 min at −20°C. Air-dried slides were then stored in a tight container at −20°C until use (35). The slides were dipped in xylene for 1 h at 60°C and then immersed in fresh xylene (30 min at 37°C) and rehydrated through graded alcohol (100%, 75%, 50%, and 25% ethanol diluted in water). Cells were rendered permeable by incubation for 10 min at room temperature in 0.02 M HCl and for 90 s in 0.01% Triton X-100. Then, proteins were depleted by incubation with proteinase K (Sigma-Aldrich) (2 μg/ml, for 30 min at 37°C). The proteinase was inactivated by addition of 0.2% glycine (Sigma-Aldrich). Free DNA in the cells was fixed with 4% buffered formalin to prevent washing off. Slides were washed in PBS and dehydrated through graded alcohol (25%, 50%, 75%, and 100%) and air dried.

Preparation of tissue for histology and microbiology. For histological study, we removed from the fifth mouse of each group the lung, spleen, and liver and immersed them in 10% buffered formalin (Fisher) for 24 h prior to embedding in paraffin. Serial 3- to 4-μm sections from each tissue specimen of mice and sheep were cut, placed on silane-coated microscope slides (Sigma-Aldrich), and incubated in an oven at 50 to 60°C for 36 to 48 h to ensure maximum tissue adhesion on the slide. The first three serial sections were subjected to hematoxylin and eosin, auramine rhodamine, and ZN staining, respectively. Auramine rhodamine staining was performed using the TB *Fluorostain* kit (Polyscience, Inc.).

Preparation of tissue for mycobacterial DNA and rRNA detection by in situ assays. For nucleic acid staining, tissue sections were processed in coplin jars as described for *M. tuberculosis* study by Hernandez-Pando and colleagues (18). Briefly, sections were deparaffinized (18 h at 60°C in xylene) and then immersed in fresh xylene (30 min at 37°C) and rehydrated through graded alcohol (100%, 75%, 50%, and 25% ethanol diluted in water). Cells were rendered permeable by incubation for 10 min at room temperature in 0 · 02 M HCl and for 90 s in 0.01% Triton X-100. Then, proteins were depleted by incubation with proteinase K (Sigma-Aldrich) (5 to 20 μg/ml for 30 min at 37°C). The proteinase was inactivated by addition of 0.2% glycine (Sigma-Aldrich). Endogenous alkaline phosphatase was inactivated by treatment with 20% acetic acid for 15 s. Free DNA in the cells was fixed with 4% formaldehyde to prevent washing off. Slides were washed in PBS, dehydrated through graded alcohol (25%, 50%, 75%, and 100%), and air dried.

Preparation of DIG-labeled probes. Digoxigenin (DIG)-labeled double-stranded DNA probes for the *Mycobacterium avium* subsp. *paratuberculosis*-specific insertion element IS*900* were synthesized according to the manufacturer's instructions using the PCR DIG probe synthesis kit (Roche). Primer sequences and PCR conditions used for probe synthesis are provided in Table 1. The PCR was performed in a total volume of 50 μl containing 5 μl of *Mycobacterium avium* subsp. *paratuberculosis* strain K10 template DNA (10 ng/μl) and 0.5 μM of each primer. Amplified products were purified using QIAGEN PCR purification kit (QIAGEN) and visualized after electrophoresis at 80 V for 90 min in a 2% agarose gel containing ethidium bromide. To confirm that the probes were synthesized correctly, amplified products were hybridized to genomic DNA of *Mycobacterium avium* subsp. *paratuberculosis* strain K10 and to PCR amplicons of primer pair L1/L2 (Table 1) blotted onto a nitrocellulose membrane (Hybond+; Amersham Biosciences) according to the manufacturer's

TABLE 2. rRNA-based probes used for in situ hybridization

Probe	rRNA probe sequence (5′–3′)	Hybridization temp (°C)	Reference
M. avium	MAVP187ssu: TGC GTC TTG AGG TCC TAT CC (16S)	40	49
	MAVP515lsu: TGT CCA TGC ATG CGG TTT (23S)	40	
M. tuberculosis	MTB226: CCA CAC CGC TAA AGC GC (16S)	38	48
	MTB187: TGC ATC CCG TGG TCC TAT CC (16S)	38	
	MTB770: CAC TAT TCA CAC GCG CGT (23S)	38	
Eubacteria	EUB338: CTG CTG CCT CCC GTA GGA GT (16S)	40	2

instruction. The DNA concentration of the purified product was estimated using spectrometer, and the probe was used at a concentration of 1 ng/μl in the hybridization procedure.

DIG-labeled double-stranded IS*900* probe in situ hybridization. Hybridization was performed as described by Hulten and colleagues (21). The tissue sections processed for nucleic acid staining were hybridized with denatured double-stranded DIG-labeled probe (1 ng/μl) in hybridization buffer (50% deionized formamide, 2× SSC [1× SSC is 0.15 M NaCl plus 0.015 M sodium citrate], 10% dextran sulfate, 0.25 μg/μl of yeast tRNA [Sigma-Aldrich], 0.5 μg/μl of denatured salmon sperm DNA [heated for 10 min at 95°C and chilled for 10 min] [Sigma-Aldrich], and 1× Denhardt's solution [Sigma-Aldrich]). The probe was boiled for 10 min and cooled on ice for 10 min before application. The sections with the probe were sealed with Frame-Seal incubation chambers (MJ Research, Inc.), heated for 10 min at 95°C, and chilled for 10 min. The hybridization was performed overnight at 37°C on a flat block of a thermocycler (MJ Research, Inc.). The washing steps included washes with 2× and 1× SSC at room temperature for 15 min in each and with 0.3× SSC for 15 min at 40°C, followed by another wash at room temperature for 15 min with 0.3× SSC. This was followed by blocking of nonspecific sites with blocking buffer (3% bovine serum albumin, 100 mM Tris [pH 7.5], 150 mM NaCl, 0.3% Triton X-100) at room temperature for 30 min. Fresh blocking buffer containing a 1:300 dilution of antidigoxigenin–alkaline phosphatase Fab fragments (Roche) was added to the slides, and the slides were incubated at room temperature for 2 to 3 h. The slides were then washed with buffer 1 (100 mM Tris [pH 7.5], 150 mM NaCl, 0.3% Triton X-100) for 15 min, followed by another wash with buffer 2 (100 mM Tris [pH 9.5], 150 mM NaCl, 50 mM MgCl2) for 15 min. The slides were then incubated with 5-bromo-4-chloro-3-indolylphosphate-2-(4-iodophenyl)-3-(4-nitrophenyl)-5- phenyltetrazolium chloride (Roche) (75 μl per 10 ml buffer 2 and 0.2 mg of levamisole [Sigma-Aldrich] per ml) in the dark at room temperature for 4 to 12 h. The reaction was stopped by washing the slides in distilled water. The slides were counterstained with nuclear fast red (Sigma-Aldrich), mounted with Cytoseal 60 (Richard-Allan Scientific), and examined under magnification ×1,000 with a bright-field microscope.

Indirect in situ PCR detection of internal fragment of IS*900*. Sections processed for nucleic acid staining were subjected to PCR in order to amplify a 400-bp sequence of the IS*900* insertion element containing the probe target sequence. The PCR was carried out by incubating the 4-μm section with 165 μl of PCR mixture (each 50 μl of PCR mixture contained 1× reaction buffer [AmpliTAq Gold; Applied Biosystems], 3 mM $MgCl_2$, 200 μM of deoxynucleoside triphosphate, and 0.5 μM of each primer for IS*900* (L1 and L2) and 12 U *Taq* DNA polymerase [AmpliTAq Gold; Applied Biosystems]) sealed with Frame-Seal incubation chambers (MJ Research, Inc.) on a flat block of a thermocycler (MJ Research, Inc.). Primer sequences and PCR conditions used are found in Table 1. After PCR, sections were washed in PBS for 1 min at room temperature and then subjected to in situ hybridization with the internal digoxigenin-labeled double-stranded IS*900* probe as described above.

rRNA-specific oligonucleotide probe in situ hybridization. Sequences of oligonucleotide probes used in this study are given in Table 2. Probes were obtained from Integrated DNA Technologies, Inc., and were labeled at the 5′ and 3′ ends with either 6-carboxyfluorescein, Cy3, or Texas Red. For in situ hybridization with rRNA-specific oligonucleotide probes, sections were subjected to hybridization as described by St Amand et al. (49) except that tissue sections were permeabilized by incubation in xylene overnight and digestion with proteinase K (Sigma-Aldrich) (5 to 20 μg/ml, for 30 min at 37°C). Smears of cultures and tissue sections processed for rRNA staining were then hybridized with probes at a final concentration of 1 ng/μl in the hybridization buffer (900 mM NaCl, 20 mM Tris [pH 8.0], 0.01% sodium dodecyl sulfate, and 20% formamide) in an MJ Research, Inc., flat block thermocycler. Hybridization temperatures for each probe are specified in Table 2. Following hybridization, the slides were washed with 225 mM NaCl, 5 mM EDTA, 0.01% sodium dodecyl sulfate, and 20 mM Tris (pH 8.0) for 20 min at either 39°C for *M. tuberculosis*-specific probes or 41°C for *M. avium* complex-specific and eubacterial probes. The slides were then immersed briefly in cold 20 mM Tris (pH 8.0) in order to remove excess salt. Colorimetric hybridization of the 6-carboxyfluorescein-labeled oligonucleotide probes was carried out as described by St Amand et al. (49) except that anti-fluorescein-labeled alkaline phosphatase Fab fragments (Roche) were used in a 1:300 dilution. Colorimetric signals were visualized using a Zeiss Axioscope microscope (Carl Zeiss). Tissue sections subjected to fluorimetric hybridization were mounted with Citifluor (Electron Microscopy Sciences) antifading reagent and for examination under an epifluorescence microscope (Nikon Eclipse E600 microscope).

Controls for nucleic acid staining assays. The specificity control for IS*900* in situ hybridization, indirect in situ PCR (IS PCR), and rRNA-based probes consisted of performing the whole procedure with tissue sections from uninfected *and M. tuberculosis*-infected mice. Additional negative controls included hybridizing test samples with unlabeled probe targeting IS*900* to determine whether aggregation of colorimetric dye could interfere with signal interpretation. For the rRNA hybridization study, uninfected and *M. tuberculosis*-infected mice served as negative controls, a universal eubacterial probe (EUB338) was used as an internal positive control, and *M. tuberculosis*-specific oligonucleotide probes (MTB226, MTB187, and MTB770) applied to *Mycobacterium avium* subsp. *paratuberculosis*-infected tissue served as an additional negative control.

Microscopic and photographic details. To look for organisms, we first studied hematoxylin-and-eosin-stained slides by using a Zeiss Axioscope microscope (Carl Zeiss), to mark areas of inflammatory infiltrates. Corresponding sites on the slides stained with ZN were examined by light microscopy (Zeiss Axioscope microscope), using 40× and 100× objectives and a 10× eyepiece, resulting in total magnifications of ×400 and ×1,000, respectively, to visualize mycobacterial forms. To further characterize bacterial forms, auramine rhodamine-stained tissue sections and smear of in vitro-grown *Mycobacterium avium* subsp. *paratuberculosis* and *M. bovis* BCG were also examined under magnifications ×400 and ×1,000 using an epifluorescence microscope (Nikon Eclipse E600 microscope) equipped with a Retiga digital camera (QImaging Corporation). We then used captured images from this analysis to determine the visual attributes of bacillary forms. Using Emplix Imaging Northern Eclipse software (Empix Imaging, Inc.), we determined morphometric parameters for 31 *M. tuberculosis* bacilli in murine tissue, 30 *M. bovis* BCG organisms in a smear of log-phase in vitro culture, 37 *Mycobacterium avium* subsp. *paratuberculosis* bacilli, and 25 *Mycobacterium avium* subsp. *paratuberculosis* coccobacilli in murine tissue, 52 *Mycobacterium avium* subsp. *paratuberculosis* bacilli in ovine tissue, and 30 *Mycobacterium avium* subsp. *paratuberculosis* organisms in a smear of log-phase in vitro culture. These included the following: (i) the length of the bacilli, defined as the longest line through an object parallel to its orientation, (ii) the width, defined as the longest line through an object that is perpendicular to its orientation, (iii) the area, defined as the integrated zone of signal, and (iv) the shape factor, defined as $4\pi \times \text{area/perimeter}^2$. The shape factor serves as a measure of circularity and is designed to produce a result of 1 for a perfect circle, 0.78 for a square, and 0.50 for a "4 × 1" rectangle. All color images were taken using Zeiss Axioscope microscopes equipped with an Axiocam MR digital camera (Carl Zeiss).

To directly compare the capacity to detect organisms with rRNA-based staining versus the ZN stain, we enumerated bacillary forms by examining 100 fields of ×1,000 oil immersion fields of sequential sections from the same blocks of liver and spleen. Numbers were compiled independently and were compared as organisms detected per granuloma by the two methods.

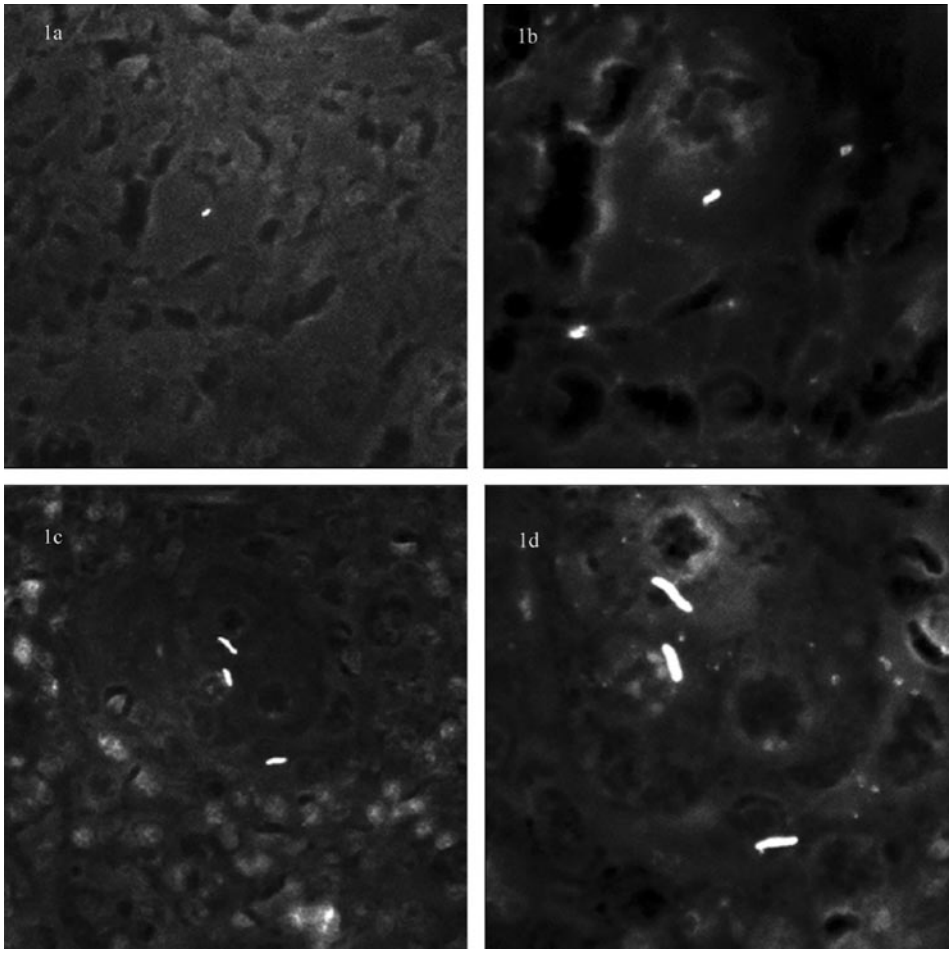

FIG. 1. Comparison of morphometric perception of *M. tuberculosis* and *M. avium* subsp. *paratuberculosis* under 40× and 100× objectives. Auramine-rhodamine-stained sections of spleen from *M. avium paratuberculosis*- and *M. tuberculosis*-infected mice. (a) Under a 40× objective, providing ×400 total magnification, individual *M. avium paratuberculosis* forms are difficult to distinguish from artifacts. (b) Under an oil immersion objective, with total magnification ×1,000, individual *M. avium paratuberculosis* organisms are detectable. (c) In contrast, individual *M. tuberculosis* bacilli can be seen using a 40× objective and are further resolved using oil immersion (d).

RESULTS

Characterization of bacterial burden in model infections. Counts of CFU for livers and spleens from mice infected intraperitoneally with *Mycobacterium avium* subsp. *paratuberculosis* revealed 10^2 to 10^3 organisms per spleen and undetectable bacterial infection in the liver. This translated into less than 10 CFU per mg of spleen tissue. At this tissue burden, no mycobacteria could be detected in a thorough microscopic examination of a 4-μm acid-fast-stained tissue section using either ZN or auramine rhodamine-based study. In contrast, intravenous infection with *Mycobacterium avium* subsp. *paratuberculosis* and *M. tuberculosis* generated CFU that were approximately 2 logs higher, such that the bacterial burden was consistently between 10^2 and 10^3 CFU/mg of tissue. For studies of detection of *Mycobacterium avium* subsp. *paratuberculosis* presented below, the mean number of bacteria per mg of splenic tissue was 396 (standard errors of the mean [SEM] = 193). At this bacterial burden, approximately 5 to 10 mycobacteria were visualized per 25 oil immersion fields examined. Samples of this tissue were thus considered to represent paucibacillary mycobacterial infection and were used in the in situ studies detailed below.

Cell wall-based staining methods for detection of mycobacteria in tissue samples. Examination of ZN-stained sections of samples from paucibacillary murine infections revealed that individual mycobacteria could only be visualized by careful examination under ×1,000 oil immersion. Occasional aggregates of several mycobacteria were noted and could be detected under magnification ×400, consistent with our experience with sections of multibacillary Johne's disease, where aggregates of mycobacteria are readily visualized under magnification ×400. By comparison, examination of tissue samples derived from *M. tuberculosis*-infected mice revealed that individual mycobacteria were detectable using magnification ×400. When tissue samples from both *M. avium* subsp. *paratuberculosis*- and *M. tuberculosis*-infected mice were subjected to auranime rhodamine staining, examination under magnification ×400 was sufficient to visualize fluorescent signals for both organisms. However, while *M. tuberculosis* signals could

TABLE 3. Morphometric parameters of mycobacterial signals: dimensions and shape of bacillary forms in tissue

Bacterium	State	Length (μm) (±SEM)	Width (μm) (±SEM)	Area (μm^2) (±SEM)	Shape factor[a] ± SEM
M. tuberculosis	In vitro	3.10 ± 0.11	0.88 ± 0.03	1.92 ± 0.11	0.44 ± 0.01
	Murine infection	3.59 ± 0.15	0.99 ± 0.02	2.26 ± 0.09	0.41 ± 0.02
Mycobacterium avium subsp. *paratuberculosis*	In vitro	1.54 ± 0.08	0.74 ± 0.03	0.81 ± 0.07	0.62 ± 0.01
	Ovine infection	1.66 ± 0.08	1.00 ± 0.05	1.25 ± 0.10	0.69 ± 0.02
	Murine infection	1.59 ± 0.06	0.91 ± 0.03	1.03 ± 0.07	0.67 ± 0.01

[a] Shape factor = $4\pi \times$ area/perimeter^2.

be recognized as mycobacteria based on their morphology, signals derived from *M. avium* subsp. *paratuberculosis* were half as long and less rod-like; therefore, it was difficult to distinguish bacterial signals from artifact (Fig. 1a and c). Thus, for both ZN and auramine-based visualization, isolated *M. avium* subsp. *paratuberculosis* organisms were only reliably visualized under ×1,000 oil immersion (Fig. 1b and d). To understand the need for magnification-×1,000 microscopy, we digitally captured mycobacterial signals and estimated their morphometric parameters. By measuring mycobacterial forms from these two infections, we could determine that *M. avium* subsp. *paratuberculosis* signals were shorter (1.59 μms ± 0.06 SEM versus 3.59 μm × 0.15 SEM), of a smaller area (1.03 × 0.07 μm^2 versus 2.26 ± 0.09 μm^2), and had a higher shape factor (0.67 ± 0.01 versus 0.41 ± 0.02) than *M. tuberculosis* signals (all *P* values were <0.01; see Table 3). Measuring *M. avium* subsp. *paratuberculosis* in ovine samples and in vitro cultures provided the same estimates as murine samples (Table 3). Additionally, for mice with few rod-shaped forms, we also observed smaller coccobacillary forms (Fig. 2); these forms were 1.12 μm (SEM = 0.07) in length by 0.78 μm (SEM = 0.06) in width, yielding an average area of just 0.63 μm^2 (SEM = 0.08).

Sensitivity and specificity of IS*900* in situ hybridization (ISH) and indirect IS PCR. Microscopic analysis of tissue

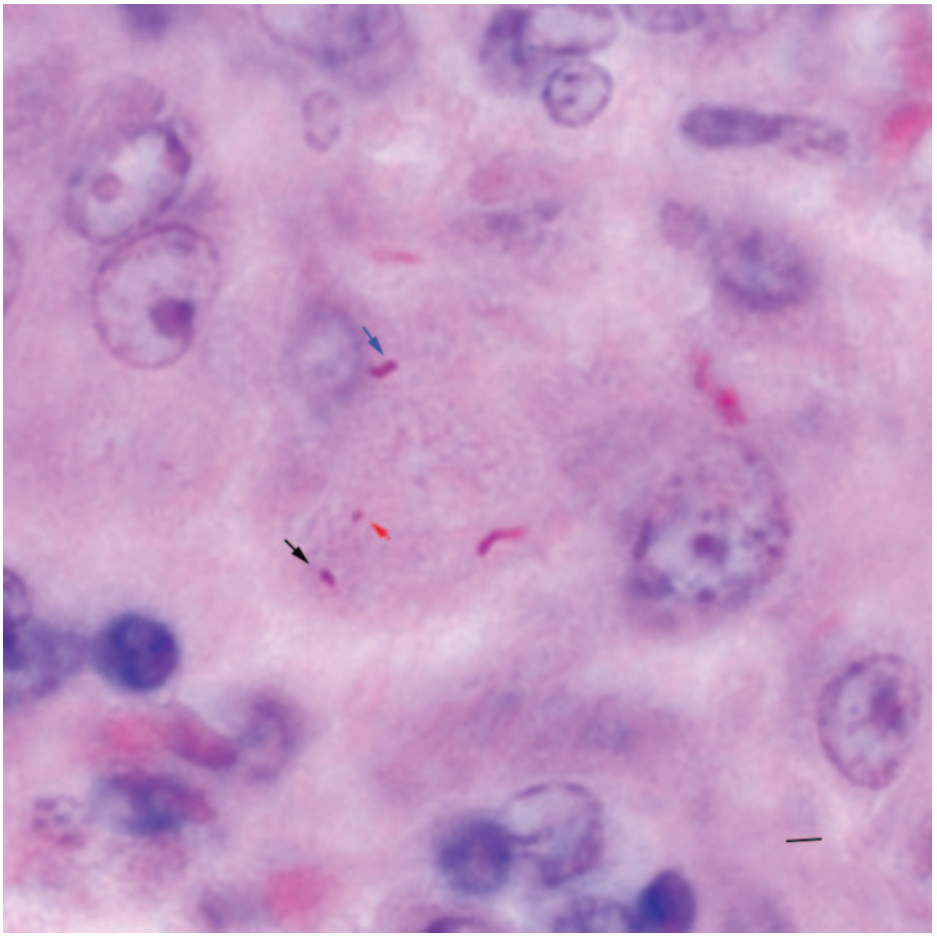

FIG. 2. Morphologically variable forms of *M. avium paratuberculosis* in tissue. Ziehl-Neelsen-stained section of a liver from an *M. avium paratuberculosis*-infected mouse showing bacillary (blue arrow), coccobacillary (black arrow), and coccoid forms (red arrow) of the organism. Bar, 2 μm; magnification, ×1,000.

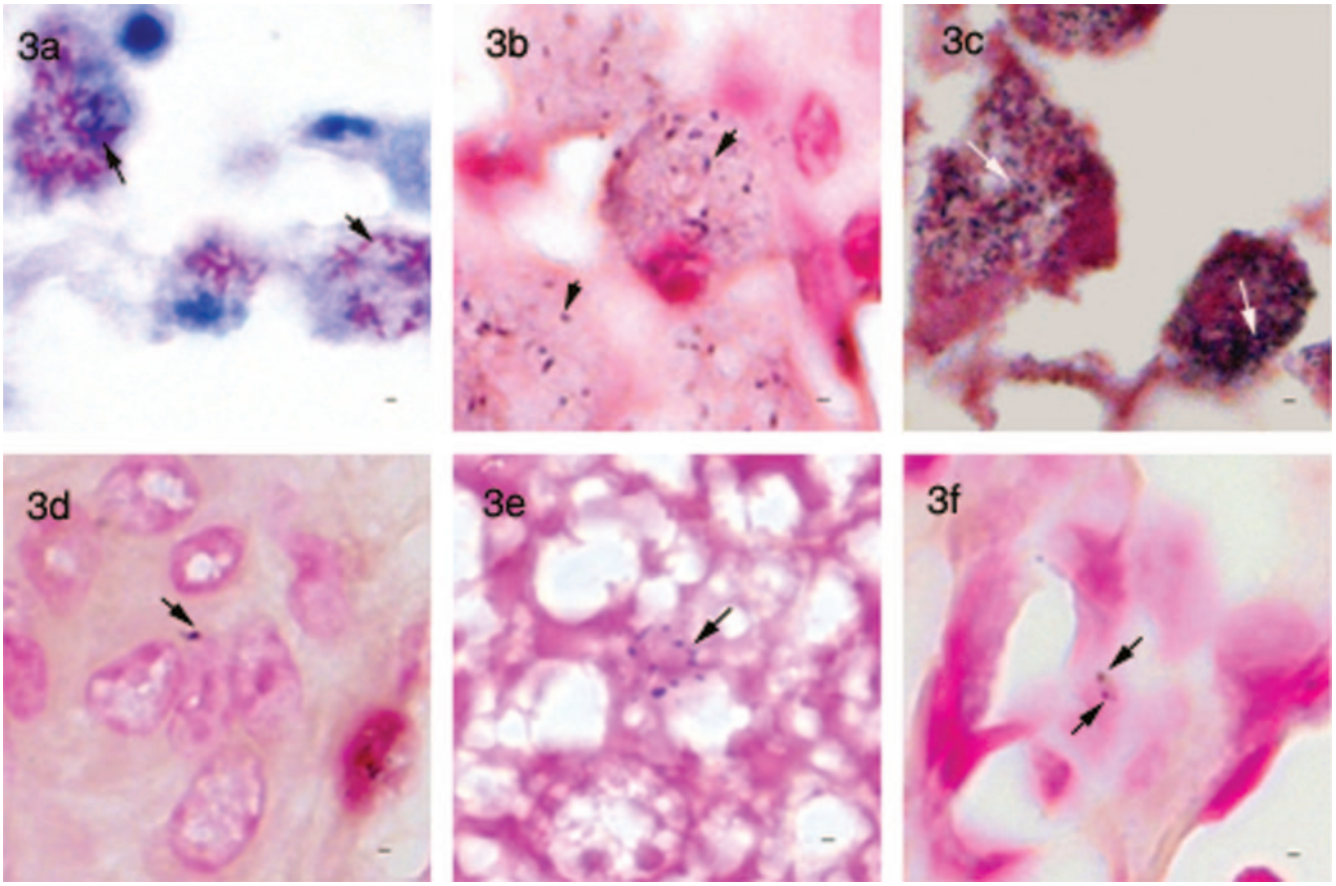

FIG. 3. IS*900*-based in situ staining assays. (a) Ziehl-Neelsen-stained tissue section of ovine intestinal tissue showing a large number of mycobacteria in macrophages (arrows). (b) IS*900*-probe-based in situ hybridization of a sequential section of the same tissue, showing positive labeling (arrow) but a reduced number of signals compared to the Ziehl-Neelsen-stained section. (c) Indirect in situ PCR for IS*900* of the same sample showing granular signals (arrows) and sensitivity comparable to that with Ziehl-Neelsen staining. (d) Section of liver from an *M. avium paratuberculosis*-infected mouse showing positive signal (arrow) by IS900-probe-based in situ hybridization. (e) Section of liver from an uninfected mouse and (f) section of lung from a mouse infected with *M. tuberculosis* showing nonspecific signals with the IS*900*-probe-based in situ hybridization method. Bar, 1 μm; magnification, ×950.

samples from Johne's sheep subjected to direct hybridization with the IS*900* probe showed variable shapes of signals ranging from rods to undefined shapes in areas found to be positive by ZN staining (Fig. 3b). However, the sensitivity, as estimated by comparing the number of positive signals across the two modalities, was much lower by IS*900* ISH than by ZN staining (Fig. 3a and b). To increase the sensitivity, we also employed indirect IS PCR, where the tissue target is first subjected to in situ amplification, before probing for the IS*900* element. Indirect IS PCR provided sensitivity comparable to that of ZN staining, but signals were mostly granular in appearance (Fig. 3c), as has been described by Sanna et al. (40). Application of both of these methods to tissue samples from *M. avium* subsp. *paratuberculosis*-infected mice resulted in the appearance of signals resembling the specific signals (Fig. 3d); however, similar signals were observed in uninfected mice and in *M. tuberculosis*-infected tissue (Fig. 3e and f). To determine the cause of these nonspecific signals, we repeated this process using an IS*900* probe without DIG; tissue samples from ovine naturally infected with *M. avium* subsp. *paratuberculosis* now failed to produce these signals, indirectly suggesting that they resulted from nonspecific binding of the IS*900* probe, as has been described elsewhere (49).

Sensitivity and specificity of rRNA ISH. Morphology of signals derived by rRNA staining of *M. avium* subsp. *paratuberculosis* in mouse tissue was consistent with that of signals visualized in smears of *M. avium* subsp. *paratuberculosis* cultures. A preliminary comparison of colorimetric signals observed in ovine tissue with those for Johne's disease suggested that the distribution of acid-fast bacilli, as revealed by ZN staining, was similar to the number of bacillary signals observed with rRNA in situ hybridization. To quantitatively compare the sensitivities of these two methods in paucibacillary infection, ISH signals and acid-fast bacilli in the same area of serial tissue sections of liver and spleen from mice infected with *M. avium* subsp. *paratuberculosis* were independently enumerated (Fig. 4a and b), revealing that the sensitivities of the two methods were comparable (ZN = 64 bacilli/45 granulomas; ISH = 53 bacilli/45 granulomas; median of 1 bacillus per granuloma by both methods; difference not significant). To determine the specificity of the rRNA-based ISH method, probes specific for *M. tuberculosis* were applied to tissue sections from mice in-

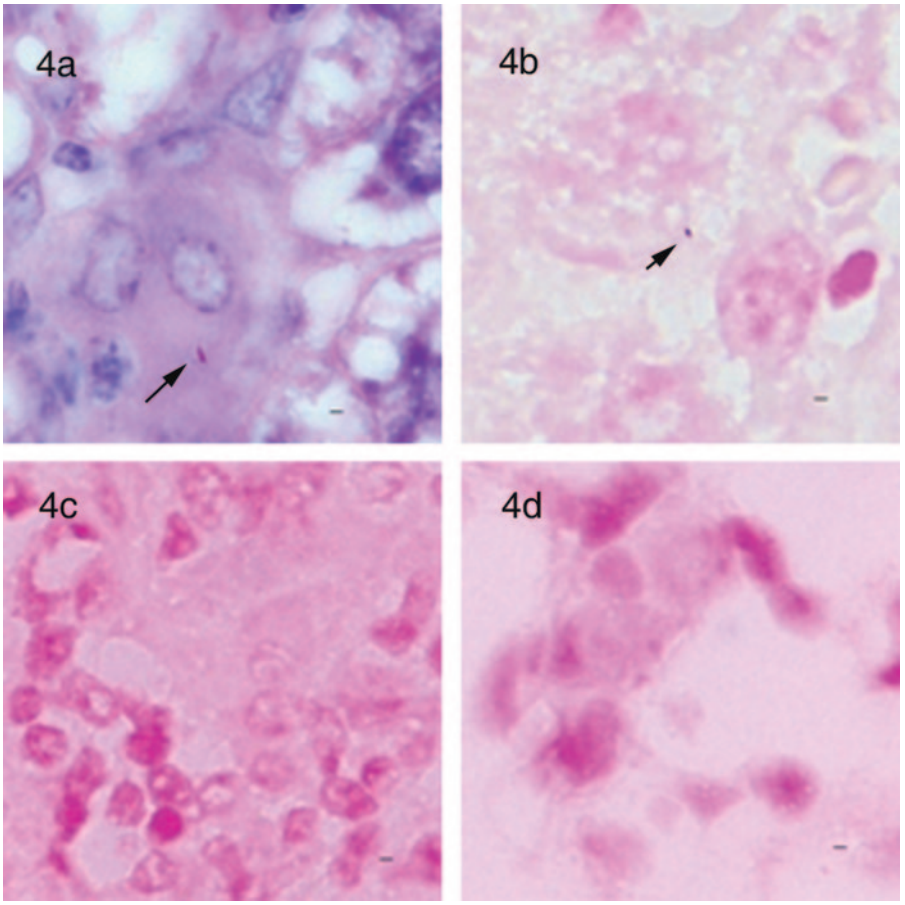

FIG. 4. rRNA-based in situ hybridization. (a) Ziehl-Neelsen-stained section of liver from an *M. avium paratuberculosis*-infected mouse showing an individual bacillary form in a granuloma. (b) In situ hybridization with *M. avium* complex-specific rRNA probes (MAVP187ssu and MAVP515lsu) on a sequential section from the same block revealing a positive signal (arrow). (c) *M. tuberculosis*-specific oligonucleotide probes applied to *M. avium paratuberculosis*-infected mouse tissue did not generate signals. (d) *M. avium* complex-specific oligonucleotide probes applied to *M. tuberculosis*-infected mouse tissue did not generate signals. Bar, 1 μm; magnification, ×1,000.

fected with *M. avium* subsp. *paratuberculosis* and, conversely, the *M. avium* probes were applied to tissue sections from uninfected and *M. tuberculosis*-infected mice. In both cases, no blue-purple precipitate was evident in any of these tissues (Fig. 4c and d). The absence of nonspecific signals in the control tissues by this assay allowed unequivocal interpretation of rod and coccoid-like signals when they were observed in the test samples. As expected, this assay also failed to detect *M. avium* subsp. *paratuberculosis* in tissue sections obtained from mice harboring less than 10 CFU/mg of tissue that were negative by acid-fast staining.

Fluorescence in situ hybridization using fluorescence-labeled, rRNA-targeted probes provided sensitivity and specificity comparable to those of the colorimetric method. Although some background autofluorescence was useful to localize the signals within tissue sections, it generally decreased the signal-to-noise ratio and hampered detection of specific fluorescent signals.

DISCUSSION

The results presented in this study demonstrate that *M. avium* subsp. *paratuberculosis* infection of tissue can be detected by microscopic methods, subject to bacterial burden, and demonstrate the limitations of various staining and visualization methods advanced as being superior to ZN staining. Our results are consistent with that for most bacteria, where oil immersion is essential in achieving sufficient resolution to properly visualize bacterial forms. In the specific case of mycobacteria, while sputum examination of fluorochrome stained smears employs magnification ×250 to ×400 for screening followed by confirmation with oil immersion, ZN-stained smears require examination under oil immersion when looking for *M. tuberculosis* (9). By comparison, *M. avium* subsp. *paratuberculosis* organisms are smaller and more elliptical, translating into a greater diagnostic challenge, especially in tissue samples. Our microscopic observations, supported by considerations of size and geometry, lead us to conclude that single *M. avium* subsp. *paratuberculosis* bacilli are essentially undetectable under magnification ×400.

An important consideration when interpreting these results is whether these experimental infections adequately modeled the process under study. Since neither Johne's nor Crohn's diseases result from parenteral inoculations of live bacteria, our infections are clearly not models of pathogenesis. How-

ever, certain aspects of our model infections concurred with our understanding of mycobacterial diagnosis. First, microscopic examination of sheep with histopathologic grade 3c (paucibacillary) Johne's disease reveals either no bacteria or a few scattered organisms (33); therefore, our experimental infections resulted in a similar diagnostic challenge. Second, bacillary forms measured from murine infections had the same size and shape as organisms seen in natural ovine disease and as in vitro-grown organisms. Third, experience from *M. tuberculosis* indicates that sputum samples with less than 10,000 bacilli per ml are typically microscopy negative (1, 26), consistent with our CFU determinations where infections with less than 10 *M. avium* subsp. *paratuberculosis* per mg of tissue (10,000 bacteria per gram) were microscopy negative but culture positive. It is recognized that our model infections of "sterile organs" did not replicate the challenges faced when examining intestinal tissue, where high quantities of enteric bacteria populate the lumen and can occasionally translocate into adjacent tissues when the mucosal barrier is damaged (14). However, we consider that the use of tissue with an otherwise clean background provided a simpler setting for rating the relative sensitivity of methods, and more importantly, the absence of other bacterial forms provided the optimal substrate to determine the specificity of these modalities.

To overcome the limitations of conventional ZN staining for the detection of *M. avium* subsp. *paratuberculosis* in tissues, a number of molecularly based assays have been developed, including in situ hybridization using probes targeting the IS*900* insertion element (20). In separate studies, we have shown that the IS*900* element is genomically specific for *M. avium* subsp. *paratuberculosis* (51) and that IS*900* sequences from a heterogeneous collection of *M. avium* subsp. *paratuberculosis* isolates are invariant (46). However, despite these favorable considerations, the IS*900*-based in situ probe was prone to nonspecific hybridization, compromising the utility of IS*900*-based in situ hybridization and indirect in situ PCR (49). In contrast, probes targeting rRNA provided excellent specificity, resulting in forms that were morphologically consistent with ZN-positive organisms on adjacent sections. A theoretical advantage of molecularly based assays would be the ability to detect greater numbers of organisms than are seen by ZN staining, if, as has been proposed, *M. avium* subsp. *paratuberculosis* adopts a cell wall-deficient (acid-fast-negative) form in tissue (10, 39). Unfortunately, we were not able to obtain any evidence in support of this notion with our murine infections, since enumeration of sequential sections of tissue for ZN-positive and rRNA-based ISH-positive bacilli revealed similar numbers of organisms by these two modalities.

An alternative means of increasing the sensitivity of microscopic detection involves the use of fluorescence microscopy, as has been done in the clinical mycobacteriology laboratory, where prolonged examination of slides using oil immersion objectives by light microscopy has been widely replaced by a fluorescence screening step under magnification ×400. Often described as a more-sensitive method, fluorescence microscopy is probably better considered more time efficient, since it permits the microscopist to conclude a negative result in a much shorter time frame, thereby generating fewer positive slides to confirm under oil immersion by light microscopy (47). In comparing the colorimetry-based ribosomal ISH to fluorimetry-based ribosomal ISH, the colorimetric method was preferred for confidently affirming the presence of *M. avium* subsp. *paratuberculosis* organisms and colocalizing these signals in the context of the histopathology. However, when numbers of signals were near the threshold of microscopic detection, thorough examination using oil immersion was time consuming and led to observer fatigue. The fluorimetry-based ribosomal ISH assay offered the possibility that signal detection might be achieved under magnification ×400, affording an opportunity to efficiently scan slides at this lower power. In our experience, with multibacillary ovine tissue, this fluorescence ISH-based approach appeared promising, but for paucibacillary infections, individual bacterial signals were too weak to be detectable at lower power. The intensity of signals is determined by a number of factors, specifically, the ribosomal content of cells, which is related to the metabolic state of the bacteria (24), penetration of probes inside the cells (35), and accessibility of the probes to the target sites on the ribosome (12). Since equivalent signal intensities were obtained using the eubacterial and *M. avium*-specific oligonucleotide probes, we could not determine factors that could be limiting the signal intensity. Recently, a number of groups have reported that substitution of DNA oligonucleotide probes with peptide nucleic acid (PNA) probes results in greater signal intensity in a number of bacterial species (24) due to their greater permeability through the bacterial cell wall (50) and target accessibility (3, 34). Since PNA probes have recently been described for the detection of *M. avium* complex organisms (25), the application of these newer in situ probes to tissue samples represents a promising avenue towards improved detection of *M. avium* subsp. *paratuberculosis* infection. The use of PNA probes and other newer modalities to detect *M. avium* subsp. *paratuberculosis* in tissue will gain from a thorough evaluation of their validity, with special attention to spectrum effect, prior to their application in epidemiologic studies.

ACKNOWLEDGMENTS

This work was supported by grants from Crohn's and Colitis Foundation of Canada and the Broad Medical Research Foundation. C.T. is supported by a Lloyd-Carr-Harris McGill Major Fellowship and an F. C. Harrison scholarship from the McGill Department of Microbiology and Immunology, and M.B. is a New Investigator of the Canadian Institutes of Health Research.

None of the authors has a conflict of interest or any commercial association that may pose a conflict of interest.

We thank Danielle Charlet, Elizabeth Fidalgo, and Makeda Semret for their input and suggestions.

REFERENCES

1. **Allen, J. L.** 1992. A modified Ziehl-Neelsen stain for mycobacteria. Med. Lab. Sci. **49:**99–102.
2. **Amann, R. I., W. Ludwig, and K. H. Schleifer.** 1995. Phylogenetic identification and *in situ* detection of individual microbial cells without cultivation. Microbiol. Rev. **59:**143–169.
3. **Armitage, B. A.** 2003. The impact of nucleic acid secondary structure on PNA hybridization. Drug Discov. Today **8:**222–228.
4. **Autschbach, F., S. Eisold, U. Hinz, S. Zinser, M. Linnebacher, T. Giese, T. Loffler, M. W. Buchler, and J. Schmidt.** 2005. High prevalence of *Mycobacterium avium* subspecies *paratuberculosis* IS900 DNA in gut tissues from individuals with Crohn's disease. Gut **54:**944–949.
5. **Bull, T. J., J. Hermon-Taylor, I. Pavlik, F. El Zaatari, and M. Tizard.** 2000. Characterization of IS900 loci in *Mycobacterium avium* subsp. *paratuberculosis* and development of multiplex PCR typing. Microbiology **146:**2185–2197.
6. **Bull, T. J., E. J. McMinn, K. Sidi-Boumedine, A. Skull, D. Durkin, P. Neild, G. Rhodes, R. Pickup, and J. Hermon-Taylor.** 2003. Detection and verifica-

tion of *Mycobacterium avium* subsp. *paratuberculosis* in fresh ileocolonic mucosal biopsy specimens from individuals with and without Crohn's disease. J. Clin. Microbiol. **41:**2915–2923.
7. **Chiodini, R. J., H. J. Van Kruiningen, W. R. Thayer, and J. A. Coutu.** 1986. Spheroplastic phase of mycobacteria isolated from patients with Crohn's disease. J. Clin. Microbiol. **24:**357–363.
8. **Dalziel, T. K.** 1913. Chronic intestinal enteritis. Brit. Med. J. **2:**1068–1070.
9. **Della-Latta, P.** 2004. Acid-fast staining, p. 7.2.1–7.2.4. *In* H. D. Isenberg (ed.), Clinical microbiology procedure handbook. American Society for Microbiology, Washington, D.C.
10. **Dell'Isola, B., C. Poyart, O. Goulet, J. F. Mougenot, E. Sadoun-Journo, N. Brousse, J. Schmitz, C. Ricour, and P. Berche.** 1994. Detection of *Mycobacterium paratuberculosis* by polymerase chain reaction in children with Crohn's disease. J. Infect. Dis. **169:**449–451.
11. **Forbes, B. A.** 1997. Critical assessment of gene amplification approaches on the diagnosis of tuberculosis. Immunol. Investig. **26:**105–116.
12. **Fuchs, B. M., G. Wallner, W. Beisker, I. Schwippl, W. Ludwig, and R. Amann.** 1998. Flow cytometric analysis of the in situ accessibility of *Escherichia coli* 16S rRNA for fluorescently labeled oligonucleotide probes. Appl. Environ. Microbiol. **64:**4973–4982.
13. **Greenstein, R. J.** 2003. Is Crohn's disease caused by a mycobacterium? Comparisons with leprosy, tuberculosis, and Johne's disease. Lancet Infect. Dis. **3:**507–514.
14. **Guarner, F., and J. R. Malagelada.** 2003. Gut flora in health and disease. Lancet **361:**512–519.
15. **Hall, M. C., B. Kieke, R. Gonzales, and E. A. Belongia.** 2004. Spectrum bias of a rapid antigen detection test for group A beta-hemolytic streptococcal pharyngitis in a pediatric population. Pediatrics **114:**182–186.
16. **Harris, N. B., and R. G. Barletta.** 2001. *Mycobacterium avium* subsp. *paratuberculosis* in veterinary medicine. Clin. Microbiol. Rev. **14:**489–512.
17. **Hermon-Taylor, J., M. Moss, M. Tizard, Z. Malik, and J. Sanderson.** 1990. Molecular biology of Crohn's disease mycobacteria. Baillieres Clin. Gastroenterol. **4:**23–42.
18. **Hernandez-Pando, R., M. Jeyanathan, G. Mengistu, D. Aguilar, H. Orozco, M. Harboe, G. A. Rook, and G. Bjune.** 2000. Persistence of DNA from *Mycobacterium tuberculosis* in superficially normal lung tissue during latent infection. Lancet **356:**2133–2138.
19. **Hulten, K., H. M. El Zimaity, T. J. Karttunen, A. Almashhrawi, M. R. Schwartz, D. Y. Graham, and F. A. El Zaatari.** 2001. Detection of *Mycobacterium avium* subspecies *paratuberculosis* in Crohn's diseased tissues by in situ hybridization. Am. J. Gastroenterol. **96:**1529–1535.
20. **Hulten, K., T. J. Karttunen, H. M. El Zimaity, S. A. Naser, A. Almashhrawi, D. Y. Graham, and F. A. El Zaatari.** 2000. *In situ* hybridization method for studies of cell wall deficient *M. paratuberculosis* in tissue samples. Vet. Microbiol. **77:**513–518.
21. **Hulten, K., T. J. Karttunen, H. M. El Zimaity, S. A. Naser, M. T. Collins, D. Y. Graham, and F. A. El Zaatari.** 2000. Identification of cell wall deficient forms of *M. avium subsp. paratuberculosis* in paraffin embedded tissues from animals with Johne's disease by in situ hybridization. J. Microbiol. Methods **42:**185–195.
22. **Ieven, M., and H. Goossens.** 1997. Relevance of nucleic acid amplification techniques for diagnosis of respiratory tract infections in the clinical laboratory. Clin. Microbiol. Rev. **10:**242–256.
23. **Lachs, M. S., I. Nachamkin, P. H. Edelstein, J. Goldman, A. R. Feinstein, and J. S. Schwartz.** 1992. Spectrum bias in the evaluation of diagnostic tests: lessons from the rapid dipstick test for urinary tract infection. Ann. Intern. Med. **117:**135–140.
24. **Lehtola, M. J., C. J. Loades, and C. W. Keevil.** 2005. Advantages of peptide nucleic acid oligonucleotides for sensitive site directed 16S rRNA fluorescence in situ hybridization (FISH) detection of *Campylobacter jejuni*, *Campylobacter coli* and *Campylobacter lari*. J. Microbiol. Methods **62:**211–219.
25. **Lehtola, M. J., E. Torvinen, I. T. Miettinen, and C. W. Keevil.** 2006. Fluorescence in situ hybridization using peptide nucleic acid probes for rapid detection of *Mycobacterium avium* subsp. *avium* and *Mycobacterium avium* subsp. *paratuberculosis* in potable-water biofilms. Appl. Environ. Microbiol. **72:**848–853.
26. **Marks, J.** 1974. Notes on the Ziehl-Neelsen staining of sputum. Tubercle **55:**241–244.
27. **Moss, M. T., E. P. Green, M. L. Tizard, Z. P. Malik, and J. Hermon-Taylor.** 1991. Specific detection of *Mycobacterium paratuberculosis* by DNA hybridisation with a fragment of the insertion element IS900. Gut **32:**395–398.
28. **Mulherin, S. A., and W. C. Miller.** 2002. Spectrum bias or spectrum effect? Subgroup variation in diagnostic test evaluation. Ann. Intern. Med. **137:**598–602.
29. **Mura, M., T. J. Bull, H. Evans, K. Sidi-Boumedine, L. McMinn, G. Rhodes, R. Pickup, and J. Hermon-Taylor.** 2006. Replication and long-term persistence of bovine and human strains of *Mycobacterium avium* subsp. *paratuberculosis* within *Acanthamoeba polyphaga*. Appl. Environ. Microbiol. **72:**854–859.
30. **Naser, S. A., G. Ghobrial, C. Romero, and J. F. Valentine.** 2004. Culture of *Mycobacterium avium* subspecies *paratuberculosis* from the blood of patients with Crohn's disease. Lancet **364:**1039–1044.
31. **Nayak, S. V., A. S. Shivarudrappa, and A. S. Mukkamil.** 2003. Role of fluorescent microscopy in detecting *Mycobacterium leprae* in tissue sections. Ann. Diagn. Pathol. **7:**78–81.
32. **Noordhoek, G. T., S. Mulder, P. Wallace, and A. M. van Loon.** 2004. Multicentre quality control study for detection of *Mycobacterium tuberculosis* in clinical samples by nucleic amplification methods. Clin. Microbiol. Infect. **10:**295–301.
33. **Perez, V., J. F. Garcia Marin, and J. J. Badiola.** 1996. Description and classification of different types of lesion associated with natural paratuberculosis infection in sheep. J. Comp. Pathol. **114:**107–122.
34. **Perry-O'Keefe, H., S. Rigby, K. Oliveira, D. Sorensen, H. Stender, J. Coull, and J. J. Hyldig-Nielsen.** 2001. Identification of indicator microorganisms using a standardized PNA FISH method. J. Microbiol. Methods **47:**281–292.
35. **Ramage, G., S. Patrick, and S. Houston.** 1998. Combined fluorescent in situ hybridisation and immunolabelling of *Bacteroides fragilis*. J. Immunol. Methods **212:**139–147.
36. **Ransohoff, D. F., and A. R. Feinstein.** 1978. Problems of spectrum and bias in evaluating the efficacy of diagnostic tests. N. Engl. J. Med. **299:**926–930.
37. **Romero, C., A. Hamdi, J. F. Valentine, and S. A. Naser.** 2005. Evaluation of surgical tissue from patients with Crohn's disease for the presence of *Mycobacterium avium* subspecies *paratuberculosis* DNA by in situ hybridization and nested polymerase chain reaction. Inflamm. Bowel. Dis. **11:**116–125.
38. **Ryan, P., S. Aarons, M. W. Bennett, G. Lee, G. C. O'Sullivan, J. O'Connell, and F. Shanahan.** 2002. *Mycobacterium paratuberculosis* detected by nested PCR in intestinal granulomas isolated by LCM in cases of Crohn's disease. Methods Mol. Biol. **193:**205–211.
39. **Sanderson, J. D., and J. Hermon-Taylor.** 1992. Mycobacterial diseases of the gut: some impact from molecular biology. Gut **33:**145–147.
40. **Sanna, E., C. J. Woodall, N. J. Watt, C. J. Clarke, M. Pittau, A. Leoni, and A. M. Nieddu.** 2000. In situ-PCR for the detection of *Mycobacterium paratuberculosis* DNA in paraffin-embedded tissues. Eur. J. Histochem. **44:**179–184.
41. **Sartor, R. B.** 2005. Does *Mycobacterium avium* subspecies *paratuberculosis* cause Crohn's disease? Gut **54:**896–898.
42. **Sechi, L. A., M. Mura, E. Tanda, A. Lissia, G. Fadda, and S. Zanetti.** 2004. *Mycobacterium avium sub. paratuberculosis* in tissue samples of Crohn's disease patients. New Microbiol. **27:**75–77.
43. **Sechi, L. A., M. Mura, F. Tanda, A. Lissia, A. Solinas, G. Fadda, and S. Zanetti.** 2001. Identification of *Mycobacterium avium* subsp. *paratuberculosis* in biopsy specimens from patients with Crohn's disease identified by in situ hybridization. J. Clin. Microbiol. **39:**4514–4517.
44. **Sechi, L. A., A. M. Scanu, P. Molicotti, S. Cannas, M. Mura, G. Dettori, G. Fadda, and S. Zanetti.** 2005. Detection and isolation of *Mycobacterium avium* subspecies *paratuberculosis* from intestinal mucosal biopsies of patients with and without Crohn's disease in Sardinia. Am. J. Gastroenterol. **100:**1529–1536.
45. **Semret, M., D. C. Alexander, C. Y. Turenne, P. de Haas, P. Overduin, D. van Soolingen, D. Cousins, and M. A. Behr.** 2005. Genomic polymorphisms for *Mycobacterium avium* subsp. *paratuberculosis* diagnostics. J. Clin. Microbiol. **43:**3704–3712.
46. **Semret, M., C. Y. Turenne, and M. A. Behr.** 2006. Insertion sequence IS*900* revisited. J. Clin. Microbiol. **44:**1081–1083.
47. **Somoskovi, A., J. E. Hotaling, M. Fitzgerald, D. O'Donnell, L. M. Parsons, and M. Salfinger.** 2001. Lessons from a proficiency testing event for acid-fast microscopy. Chest **120:**250–257.
48. **St Amand, A. L., D. N. Frank, M. A. De Groote, R. J. Basaraba, I. M. Orme, and N. R. Pace.** 2005. Use of specific rRNA oligonucleotide probes for microscopic detection of *Mycobacterium tuberculosis* in culture and tissue specimens. J. Clin. Microbiol. **43:**5369–5371.
49. **St Amand, A. L., D. N. Frank, M. A. De Groote, and N. R. Pace.** 2005. Use of specific rRNA oligonucleotide probes for microscopic detection of *Mycobacterium avium* complex organisms in tissue. J. Clin. Microbiol. **43:**1505–1514.
50. **Stender, H., M. Fiandaca, J. J. Hyldig-Nielsen, and J. Coull.** 2002. PNA for rapid microbiology. J. Microbiol. Methods **48:**1–17.
51. **Turenne, C. Y., M. Semret, D. V. Cousins, D. M. Collins, and M. A. Behr.** 2006. Sequencing of *hsp65* distinguishes among subsets of the *Mycobacterium avium* complex. J. Clin. Microbiol. **44:**433–440.
52. **Vinh, D. C., and C. N. Bernstein.** 2005. Crohn's disease and *M. paratuberculosis*: where's the beef? Inflamm. Bowel. Dis. **11:**1025–1027.
53. **Whittington, R. J., I. B. Marsh, P. J. Taylor, D. J. Marshall, C. Taragel, and L. A. Reddacliff.** 2003. Isolation of *Mycobacterium avium* subsp. *paratuberculosis* from environmental samples collected from farms before and after destocking sheep with paratuberculosis. Aust. Vet. J. **81:**559–563.